ELSEVIER

Il Farmaco 53 (1998) 214–223

IL FARMACO

Structural characterization and solution rotational isomerism of delapril hydrochloride, a dipeptide angiotensin-converting enzyme inhibitor

Enrico Redenti [a,*], Margherita Zanol [a], Gabriele Amari [a], Paolo Ventura [a], Giovanni Fronza [b], Alessia Bacchi [c], Giancarlo Pelizzi [c]

[a] *Chemical and Biopharmaceutical Department, Chiesi Farmaceutici SpA, Via Palermo 26/A, 43100 Parma, Italy*

[b] *CNR — Centro sullo Studio delle Sostanze Organiche Naturali, Dipartimento di Chimica, Politecnico, Via Mancinelli 7, 20131 Milan, Italy*

[c] *Dipartimento di Chimica Generale ed Inorganica, Chimica Analitica, Chimica Fisica, Centro di Studio per la Strutturistica Diffrattometrica del CNR, Viale delle Scienze, 43100 Parma, Italy*

Received 24 June 1997; accepted 23 December 1997

Abstract

The solid state structure of delapril hydrochloride was determined by single-crystal X-ray diffraction analysis (monoclinic, $P2_1$, $a=16.098(5)$, $b=10.712(3)$, $c=7.856(2)$ Å, $\beta=97.85(2)°$). The comparison between delapril and other ACE inhibitors of the same family is discussed with regard to the geometry of the phenomenological active site of the enzyme. In the solid state the amide bond conformation resulted in being *trans*, whereas, in solution, NMR spectra indicate that the molecule exists as a mixture of rotational isomers *trans* and *cis* (approximately 70:30). The free energy of activation for the hindered rotation about the amide bond was determined by line-shape analysis. The attempt to isolate possible conformational polymorphs failed, indicating that the *trans* conformation is favored when molecules pack together in the crystal.

Keywords: delapril; Dipeptides; Angiotensin converting enzyme (ACE) inhibitors; Rotational isomerism; Antihypertensive agents

1. Introduction

Delapril hydrochloride (Fig. 1), *N*-[*N*-[(*S*)-1-ethoxycarbonyl-3-phenylpropyl]-(*S*)-alanyl-*N*-(indan-2-yl) glycine hydrochloride, is an angiotensin-converting enzyme (ACE) inhibitor, synthesized by Oka et al. [1], which is actually marketed as an antihypertensive agent [2]. Like many of these dipeptide ACE inhibitors [3,4], delapril is a pro-drug; following oral administration, it is bioactivated by hydrolysis of the ethyl ester to the corresponding diacid form [5]. The action of ACE consists in removing the C-terminal dipeptide (His-Phe) from the decapeptide angiotensin I, thus releasing the vasoconstrictor octapeptide angiotensin II. Moreover, the enzyme can inactivate the nonapeptide vasodilator bradykinin by the cleavage of C-terminal dipeptide fragments. As a consequence, the inhibition of this enzyme results in the lowering of blood pressure [6]. Different types of ACE inhibitors are known, such as snake venom peptides containing C-terminal proline, sulfhydryl derivatives of the Ala-Pro dipeptide (like captopril [7], the first potent and orally active ACE inhibitor), and sulfur-free dipeptides with the general formula shown in Scheme 1. Delapril belongs to the latter class (see Fig. 1).

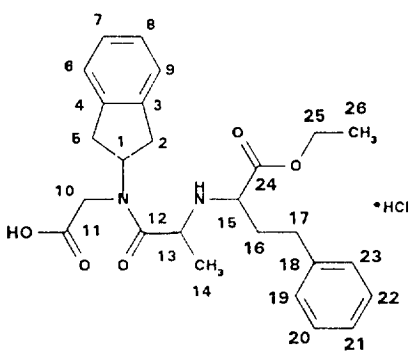

Fig. 1. Delapril hydrochloride.

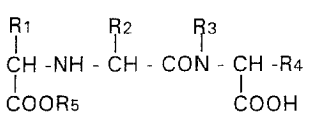

Scheme 1.

Since the structure of ACE is not known, the design of new ACE inhibiting drugs relies on the study of the correlations

* Corresponding author. Tel.: +39 521 279 438; fax: +39 521 783 321

0014-827X/98/$19.00
PII S0014-827X(98)00013-5

Table 1
Chemical diagrams of ACE inhibitors analogs to delapril whose X-ray structure has been related to activity in the literature

Enalaprilate [15]	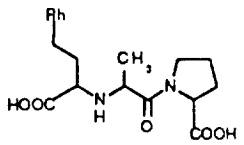	SBG107 [23]	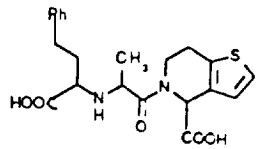
Enalapril [15]	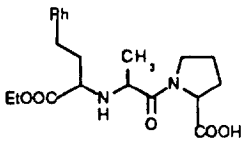	Ramiprilat [24]	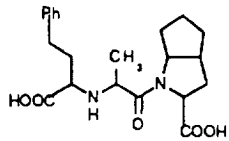
Dokmul [11]	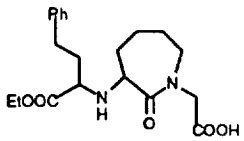	MDL27,467A [12]	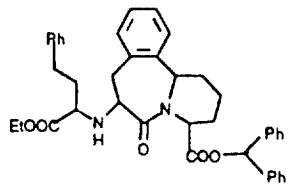
Doknas [11]	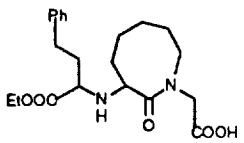	Quinapril [12]	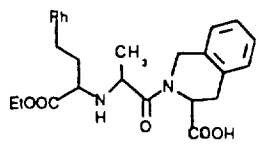
Cilazapril [22]	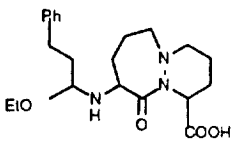	Zabicipril [25]	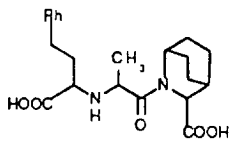

between the structure of known inhibitors and their activity (Table 1).

A study of the solid state and solution structure of delapril may contribute to a better knowledge of the steric factors governing the interactions at the active site. Although delapril possesses two chiral centers and could theoretically exist as a mixture of two pairs of racemates, only the more biologically active epimer *S,S* has been developed [1]. To date, its absolute configuration has been assigned by chemical correlation with that of enalapril, since single crystals suitable for diffractometric analysis had never been obtained (Takeda, Osaka, Japan, confidential document). The molecule also exhibits potential *cis/trans* isomerism with respect to the conformation across the amide bond. In the present paper we describe the results of a structural study of delapril hydrochloride.

Single-crystal X-ray diffraction analysis was carried out to define the stereochemistry and conformation of delapril hydrochloride across the amide bond. Simultaneously, NMR was employed for establishing which rotational isomer predominates in solution, as the rate of interchange between the *cis* and *trans* forms is slow on the NMR time scale. Lineshape analysis was applied for determining the kinetic and activation parameters. Finally, different procedures (crystallization from solvents, drying upon water dissolution) for preparing the corresponding *cis* conformational polymorph [8,9] were attempted and thermal, powder diffraction and spectroscopic (IR, solid state NMR) techniques were applied to confirm its possible existence.

2. Results and discussion

2.1. Single-crystal X-ray analysis

The single crystals were grown from ethanol. The perspective view of the molecule is reported in Fig. 2. For the sake of clarity, the atoms are numbered in a different way from that of the IUPAC notation. Its absolute configuration has been confirmed to be 13*S*,15*S*.

Ondetti et al. [7] and Cushman et al. [10] suggested a phenomenological model of the active site of ACE; since then, this model has been tested and further developed by a number of structural studies on ACE inhibiting drugs [11–13]. In the present study, attention is focused on the family of sulfur-free drugs to which delapril belongs. A schematic map of the different sites of interaction between the enzyme and a general delapril-like inhibitor is depicted in Scheme 2.

It can be seen that the pharmacophore consists of:

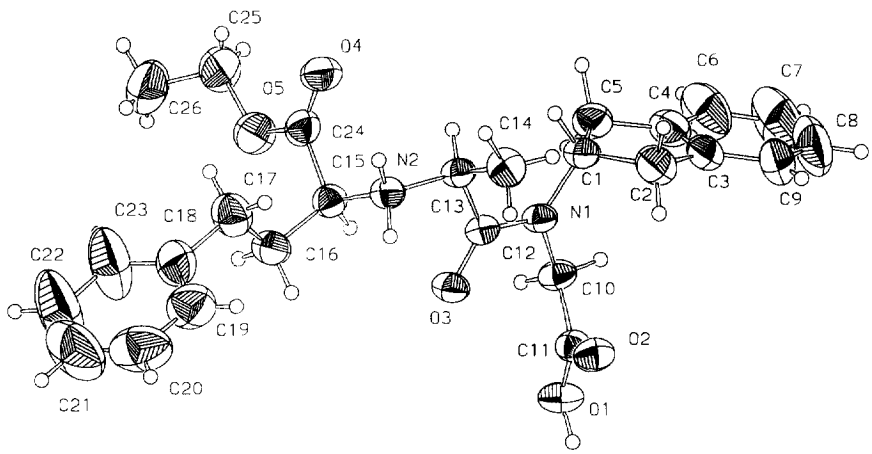

Fig. 2. ORTEP view of delapril hydrochloride. The thermal ellipsoids are drawn to the 30% probability level.

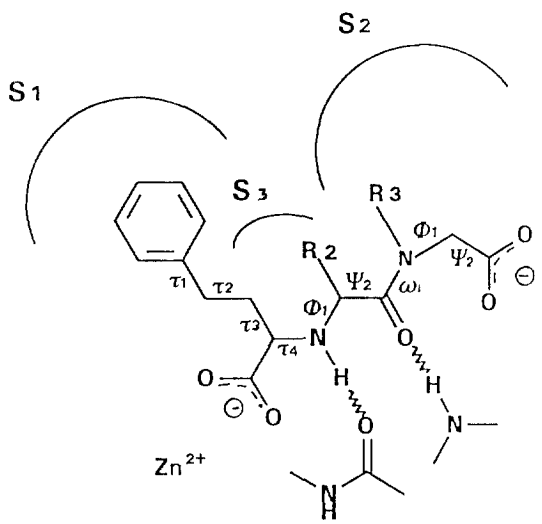

Scheme 2.

(1) a group coordinating the Zn atom present in the active site; in sulfur-free drugs this is carboxylate, in captopril-like drugs it is a –SH;

(2) a negative charge, carried by a second carboxylate, which interacts with a positive charged residue on the enzyme;

(3) the peptidic C=O, correctly positioned in order to hydrogen-bond to an enzymatic –NH;

(4) the N-terminal –NH, suitably oriented to act as a hydrogen-bond donor to an enzymatic C=O; it is not clear if the aminic group is protonated when bonded to the enzyme [3];

(5) a substituent R1 accommodated in a hydrophobic pocket of the enzyme; so far the most efficient group is phenylethyl [3];

(6) a lipophilic substituent R3; it is known that cyclic terminal amino acids (i.e. R3 fused with R4) enhance ACE inhibiting activity, probably due to favorable interactions with the hydrophobic pocket [13]; in general, molecules with bulky substituents at R3 are more active;

(7) the side chain R2; it has been shown [11] that the presence of alanine in the dipeptidic skeleton of the molecule, i.e. R2 = $-CH_3$, is important but not essential to enhance activity; in particular, it was suggested that the binding site for R2 is almost fused with the pocket accommodating R3, since the introduction of large rings linking R2 and R3 gives active compounds.

In order to optimize the above seven possible interactions with the active site, the molecular structure of the inhibitor needs to satisfy some restrictions. Since the actual spatial arrangement of the active site is not known, the study of the conformational preferences of the present class of inhibitors gives an insight into the conditions required for activity. This extrapolation is based on the assumption that the inhibitors bind to the enzyme in low-energy conformational states, closely represented by those found experimentally in solution and in the solid state. Clearly, the greater the number of available structural data, the greater the confidence that can be placed on the model. The conformation of delapril hydrochloride in the crystalline state has been examined in order to contribute to a more precise mapping of the geometric features of the inhibitor–enzyme complex. The most relevant parameters [13,14] describing delapril's molecular conformation and pharmacophore geometry are discussed here and compared with those of ten other members of the same family of ACE inhibitors. The schematic formulas of these molecules are presented in Table 1, together with literature references; the related data have been retrieved using the Cambridge Structural Database (release April 1996), querying for the fragment in Scheme 1, with R1 = phenylethyl.

The dipeptide backbone and the orientation of the phenylethyl chain can be characterized by the torsion angles defined as in Scheme 2 and listed in Table 2.

2.1.1. Terminal carboxyl (Ψ_2, Φ_2)

Examination of conformational energy maps [14] indicated that the terminal –COOH is nearly free to rotate, consequently no preferences should be observed for Ψ_2. However, for nine out of ten molecules Ψ_2 ranges between

Table 2
Representative torsion angle (deg) for delapril hydrochloride (present paper) and other ACE inhibitor analogs (retrieved from the Cambridge Structural Database)

	Ψ_2	Φ_2	Ψ_1	Φ_1	τ_1	τ_2	τ_3	τ_4
Delapril hydrochloride	155.1(3)	−61.0(4)	170.0(3)	−60.7(4)	158.2(3)	68.1(4)	−178.3(4)	93.8(6)
Enalaprilate [16]	174.572	−88.192	143.040	−59.271	167.828	64.045	178.903	−179.608
Enalapril [15]	139.688	−52.772	156.348	174.975	57.469	67.731	179.385	83.894
Dokmul [11] (CSD Refcode) [a]	168.627	−78.190	165.646	−80.912	167.892	−76.742	−170.846	13.293
Doknas [11] (CSD Refcode)	165.191	−69.945	158.992	−66.338	151.279	66.375	−177.087	−88.974
Cilazapril [22]	30.908	−82.203	174.231	−76.109	172.220	−75.063	163.645	−108.905
SBG107 [23]	168.988	−93.589	151.228	−63.944	160.762	60.793	175.758	11.924
Ramiprilat [24]	167.287	−81.379	130.664	−56.474	157.532	66.481	173.480	−91.947
MDL27,467A [12]	168.960	−93.996	158.147	−82.540	49.804	−164.983	170.246	109.786
Quinapril [12]	140.776	−52.682	172.278	−69.138	161.495	−80.422	177.707	77.907
Zabicipril [25]	163.600	−62.720	162.462	−65.161	170.214	66.813	−177.415	81.315

[a] The crystalline structure of the racemate is reported in Ref. [11]; here, only the C15(S) molecule is considered.

140° and 175°, and delapril falls well within this range. In the only outlier (cilazapril monohydrate, $\Psi_2 = -153°$) the terminal carboxyl is deprotonated. This preferential orientation could be due to common features in the crystal packings.

2.1.2. Amide bond (ω)

The amide bond is planar ($\omega = -117.8(3)°$) and adopts the biologically active *trans* configuration, which is also the most stable in solution (see below).

2.1.3. Alanine–CH_3 (Ψ_1)

In delapril the orientation of the side chain R2 is nearly perpendicular to the amide plane ($\Psi_1 = 170.0(3)°$), as predicted by previous studies which indicate that a range between 130° and 170° for Ψ_1 is essential for activity. Accordingly, within the ten delapril analogs, Ψ_1 is distributed between 130.7° and 174.2°.

2.1.4. Zinc-binding carboxylate (Ψ_1, Φ_1, τ_1)

The spatial arrangement of delapril zinc-binding carboxylate, which in the pro-drugs is esterified, is perfectly consistent with the average geometry found for the other analogs. Two exceptions are enalapril [15] and MDL27,467A hydrochloride [12]. In the former, the propylphenyl side chain and the carboxylate are permuted in their positions, as shown by the value of $\Psi_1 = 175°$; however, the corresponding active form, enalaprilate [16], is perfectly comparable with the average. In MDL27,467A hydrochloride the entire substituent at the aminic terminal of the dipeptide is rotated by roughly 120° around the N–C bond, as shown by the comparison of $\tau_1 = 50°$ with the average value of 164° determined for the other eight compounds.

2.1.5. Aromatic side chain (τ_2, τ_3, τ_4)

The suggested optimal values for τ_2, τ_3, τ_4 are, respectively, 180–240°, 180°, 90° [14]. In delapril the chain is extended ($\tau_3 = -178.3(4)°$) and the phenyl plane is nearly perpendicular to the chain plane ($\tau_4 = 93.8(6)°$), but the chain is oriented in a conformation synclinal to the C15–N2 bond ($\tau_2 = 68.1(4)°$), while the indicated minimum energy value is in the anticlinal 180–240° region. By inspecting the distribution of preferred conformations for the related compounds, it results that there are two families of rotamers clustering around $\tau_2 = -60°$ and $\tau_2 = +60°$ respectively. Both conformers have extended chains, and the terminal phenyl may choose to sit in a plane roughly either perpendicular or parallel to the chain plane.

Recalling the considerations of Thorsett et al. [11], it must be noted that it is not the single torsion angle or structural parameter which determines the energy of the binding between ACE and the inhibitor, but the drug molecule adapts its conformation in order to obtain the most favorable steric arrangement. The final structure of the enzyme–inhibitor complex will be the result of this cooperative and adaptive process. Thus, the variations in τ_2, for instance, could be compensated by torsional modifications in other parts of the molecule. To visualize and verify this principle, the X-ray structures of delapril and its ten analogs have been superimposed by least squares, minimizing the differences in the atomic coordinates referred to the molecular inertial axes, with the auxilium of the Cambridge Structural Database packages. This approach reflects the idea that no atoms will exactly coincide in the final superposition, but that the overall differences in relative orientations will be minimized; in this way the global similarities are shown up and the envelope of the active molecular shapes is obtained. At first, it was observed that enalapril [15] and MDL27,467A hydrochloride [12] did not fit the pattern common to the other molecules, due to the above-mentioned completely different orientation of the N-terminal substituent, consequently they were left out of the analysis. The final plot (Fig. 3), shows that the pharmacophore is spatially quite well-defined, and that, despite the observed variations of τ_2, the terminal aromatic ring position is preserved.

2.1.6. Conformation of the indane group

The substitution of bulkier, lipophilic groups at the C-terminus generally leads to increased activity [12]. Com-

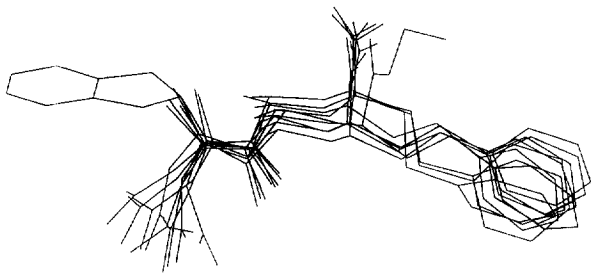

Fig. 3. Least-squares superposition of delapril and the other ACE inhibitor analogs listed in Tables 1 and 2. The invariance of the pharmacophore pattern is shown.

monly, proline or other cyclic imino acids are employed. In delapril the C-terminus is a glycine, whose nitrogen carries an indane group. The five-membered saturated ring is a flattened envelope, with C1 0.156(3) Å out of the plane defined by C2, C3, C4, and C5, which is practically coplanar with the adjacent aromatic ring, and forming a dihedral angle of 93.5(2)° with the amide bond plane. The torsion angle C10–N1–C1–C2 = −71.0(4)° describes the mutual orientation of the glycine residue and of its N-substituent.

2.1.7. Crystal packing

The hydrogen bonds O1–H···Cl$^{(i)}$ (2.984(3) Å, 165°), N2–H1···Cl (3.121(3) Å, 156°), N2–H2···O2$^{(ii)}$ (2.973(4) Å, 167°) ((i): $1-x, y-1/2, 2-z$; (ii): $1-x, y+1/2, 2-z$) characterize the crystal packing of delapril (Fig. 4). This involves $>NH_2^+$ groups and –COOH groups of molecules

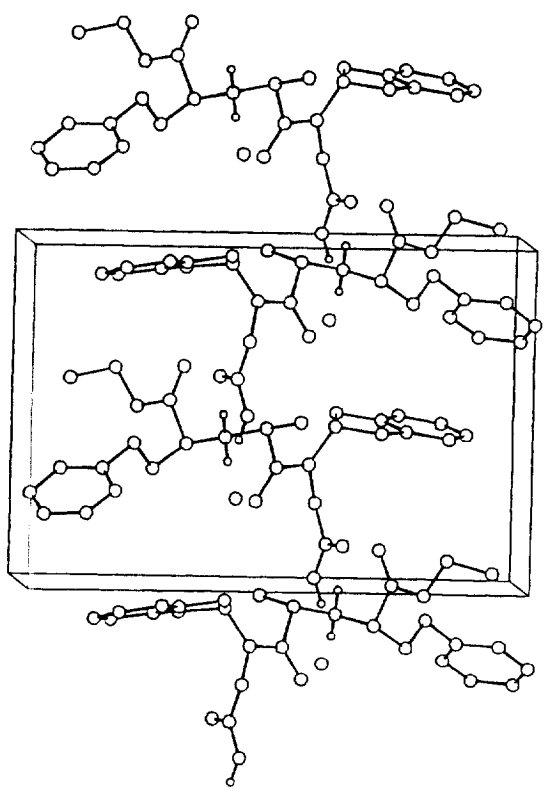

Fig. 4. Packing diagram of delapril hydrochloride.

reciprocally related by screw rotation along *b*: the interaction is direct in the case of the N2–H1···O2$^{(ii)}$ bond, and mediated by the bridging Cl anion N2–H1···Cl···H–O1$^{(ii)}$ in the second case. A chain motif is generated along *b*.

2.2. NMR study

In D_2O and DMSO-d_6, slow rotation about the amide C–N bond gives rise to paired signals for several protons and carbons of the molecule (Fig. 5). The phenomenon has been attributed to the existence of rotational isomers, as for captopril [17] and enalapril maleate [18]. The different intensities of the lines are due to the unequal populations of 1A and 1B (Scheme 3). The chemical shifts and assignments are reported in Table 3. The two rotational isomers were assigned by nuclear Overhauser effect (NOE) measurements. In order to differentiate between the NOE and cross-peaks due to chemical exchange, a phase-sensitive two-dimensional NOESY experiment was carried out at 294 K, using a mixing time of 500 ms. A strong cross-peak, observed between the H-13 and H-1 protons at 4.75 and 5.01 ppm respectively, confirms without ambiguity that the major species is the *trans* rotational conformer 1A.

On the other hand, no NOE was observed between the H-13 and H-1 resonances of the minor conformer 1B (at 4.25 and 4.95 ppm). The absence of cross-peaks with the same sign as the diagonal peaks also indicates that chemical exchange is negligible at this temperature.

The exchange rates at different temperatures were calculated by line-shape analysis as described in Section 3. As expected, the values of the rotamer populations, p_{1A} and p_{1B}, obtained from the area of the CH_3–Et group depend only slightly on the temperature (from 67:33 at 296 K to 70:30 at 340 K). The corresponding values for the free energy of activation were obtained from the Eyring equation [19]:

$$\Delta G^{\#} = aT[10.319 + \log(T/k)]$$

where $a = 4.575 \times 10^{-3}$ ($\Delta G^{\#}$ in kcal mol^{-1}). The results are summarized in Table 4.

The activation parameters were calculated from an Arrhenius plot ($r = 0.9976$):

$$\ln k = -E_a/RT + \ln A$$

where E_a is the activation energy and A the pre-exponential factor.

The enthalpy and entropy of activation were evaluated by a least-squares fit of the equation [19]

$$\ln(k/T) = -\Delta H^{\#}/RT + \Delta G^{\#}/a + 10.319$$

The values with their relative confidence limits are presented in Table 5.

The rate constant extrapolated from the Arrhenius plot at 37°C indicates a half-time for isomerism of about 5 s.

The current model of the pharmacophore for ACE inhibitors has been derived mainly by the examination of solid state conformational preferences of active compounds and on

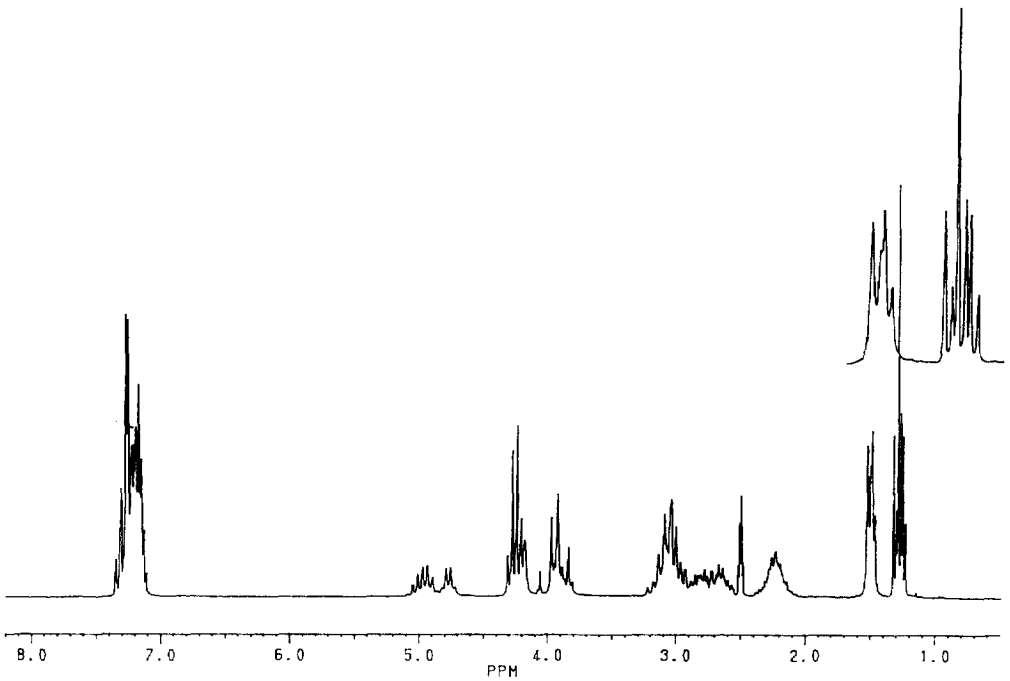

Fig. 5. ^{1}H NMR spectrum of delapril hydrochloride in DMSO-d_6 at 294 K. The methyl region expansion is reported in the right-hand corner.

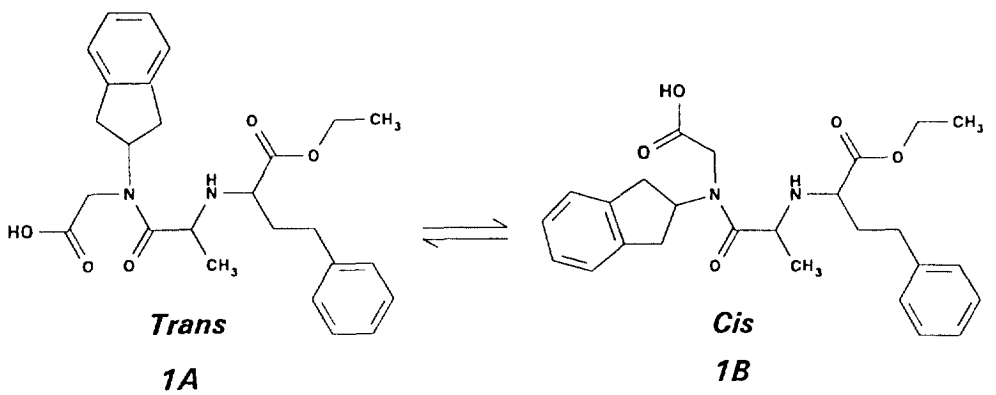

Scheme 3.

results of molecular modeling calculations [11–16,20]. The importance given to crystallographic studies is based on the rationale that the surroundings of the molecule in the crystal mimic the structured molecular environment in which the drug interacts when binding to the enzyme [21].

Delapril hydrochloride raw material, as obtained from Takeda, and the different samples I, II and III prepared for proving the existence of conformational polymorphism were analyzed by differential scanning calorimetry (DSC), FT-IR spectroscopy, powder X-ray diffractometry and solid state ^{13}C NMR. In particular, the last technique has been reported to be very useful for detecting change in conformation of functional groups in solids [8]. All the samples show the same thermal behavior (melting with decomposition at 178–181°C) and give the same diffraction pattern and IR spectra. Also, the NMR spectra were identical; they all show only a single set of peaks, corresponding to the *trans* form and in agreement with the crystallographic findings. Only the signal of carbon C10 shows an asymmetric splitting due to the residual dipolar coupling between ^{13}C and ^{14}N spins which could not be averaged by magic angle spinning [26]. Such dipolar interaction also induces a significant broadening (but not a residual splitting) of the C12 resonance, thus allowing its unambiguous assignment. The other signals were identified, at least partially, from the comparison with the ^{13}C NMR spectrum in solution and their assignments are reported in Table 6. It can be seen that several signals are shifted by 2–3 ppm to high fields on going from the solid to the solution state. These resonances are C14, C16 (or C17), C5, C2, C10, C13 and C18. These variations indicate that, in addition to the *cis/trans* equilibrium, some other conformational changes occur in solution with respect to the solid state. Generally, ^{13}C NMR high field shifts are due to the reciprocal γ-effect exerted by the nuclei along a backbone. Reasonably, in the

Table 3
^1H and ^{13}C chemical shifts δ, multiplicity M and $^1H,^1H$ coupling constants J for rotational isomers of delapril hydrochloride in DMSO-d_6 solution at 294 K

Position		δ_H (ppm)	M_H	J (Hz)	M_C	δ_C (ppm)
CH_3–Et	*cis*	1.28	t	$^3J=7$	CH_3	13.8
	trans	1.30	t	$^3J=7$		
14	*cis*	1.43	d	$^3J=6.8$	CH_3	15.6
	trans	1.46	d	$^3J=6.8$		
16	*trans*	2.0–2.5	m		CH_2	29.7
	cis	2.0–2.5				31.0
17		2.5–3.0	m		CH_2	30.4
5	*cis*	3.0–3.3	m		CH_2	35.4
	trans	3.0–3.3				35.7
2	*cis*	3.0–3.3			CH_2	35.6
	trans	3.0–3.3				36.4
15		3.90	m		CH	57.0
10	*trans*	3.95	AB syst.		CH_2	44.0
	cis	4.20				46.4
CH_2–Et		4.25	q	$^3J=7$	CH_2	61.9
13	*cis*	4.25	q	$^3J=6.8$	CH	53.0
	trans	4.76		$^3J=6.8$		52.0
1	*trans*	4.95	m		CH	56.4
	cis	5.02				56.1
20, 22		7.0–7.5	m		CH	124.2
19, 23	*trans*	7.0–7.5			CH	126.1
	cis	7.0–7.5				126.4
21		7.0–7.5			CH	126.5
6, 7, 8, 9		7.0–7.5			CH	128.2
3, 4	*trans*				C	140.1
	cis					140.2
18	*cis*				C	140.3
	trans				C	140.6
12	*cis*				C=O	167.9
	trans					168.2
11	*trans*				COOH	168.7
	cis					169.5
24	*trans*				COOEt	169.7
	cis					170.9

Table 4
Experimental results and $\Delta G^{\#}$ values for the hindered rotation of the process 1A ⇔ 1B

Probe	T (K)	k (s^{-1})	$\Delta G^{\#}$ (kcal mol^{-1})
CH_3–Et	320	0.4	19.4 [a]
	335	1.2	19.6 [a]
	345	2.2	19.7 [a]
	350	3.7	19.7 [a]
	355	5.0	19.8 [a]

[a] Considered identical within experimental errors.

Table 5
Thermodynamic parameters for the hindered rotation of the process 1A ⇔ 1B

E_a (kcal mol^{-1})	log A (s^{-1})	$\Delta H^{\#}$ (kcal mol^{-1})	$\Delta S^{\#}$ (cal mol^{-1} K^{-1})	$\Delta G^{\#}$ (kcal mol^{-1})
16.25 ± 2.09	10.69 ± 1.33	15.58 ± 0.66	-11.9 ± 1.9	19.64 ± 0.15

case of delapril, the motional averaging of the chain geometry from C13 to C17 should lead to an increase of the three bond interactions in solution.

In, conclusion, no conformational polymorphs were obtained, indicating that the *trans* conformer, which predominates in solution, is also favored when molecules pack together in the crystal.

3. Experimental

3.1. Materials

Delapril hydrochloride was licensed from Takeda (Osaka, Japan). The samples designated as I and II were prepared by crystallization at room temperature from acetone and ethanol, respectively (m.p. 178–181°C with dec.). The sample designated as III was prepared after dissolution in water and then drying at 55°C under vacuum for 6 h (m.p. 178–181°C with dec.; loss of weight <0.1%). 99.8% D_2O and DMSO-d_6 were purchased from Merck (Milan, Italy). All other chemicals were of analytical grade.

3.2. Apparatus

Infrared spectra were taken as a KBr disk on a Perkin-Elmer 2000 FT spectrophotometer (Norwalk, CT). The DSC analyses were carried out on a Perkin-Elmer DSC 7 thermal analysis system (Norwalk, CT) under nitrogen atmosphere. Each sample was heated between 50 and 220°C with a scanning rate of 10°C/min.

Single-crystal X-ray diffraction analysis was carried out at room temperature by a computer-controlled Siemens AED diffractometer (Karlsruhe, Germany) using Mo Kα ($\lambda=0.71073$ Å) radiation. Automatic peak search, centering, and indexing procedures, indicated a primitive monoclinic lattice; by the examination of systematic absences and intensity statistics the space group was determined as $P2_1$. Relevant details concerning the data collection and structure determination are collected in Table 7. No crystal decay was observed. The intensity data were processed with a peak-profile analysis procedure and corrected for Lorentz and polarization effects. The phase problem was solved by direct methods, using SIR92 [27]. A full-matrix least-squares refinement was carried out with SHELXL-93 (G. Sheldrick, University of Göttingen, Germany, 1993) on F^2, using all unique data. Anisotropic thermal displacement parameters were refined for all non-hydrogen atoms. The H atoms bonded to N1 and O1, considered potential H-bond donors, those bonded to the asymmetric carbons C13 and C15, and

Table 6
DMSO-d_6 solution and solid state ^{13}C NMR chemical shifts of *trans*-delapril hydrochloride

Assignment	δ(solid)	δ(solution)
CH_3–Et	13.6	13.8
C14	18.3	15.6
C16 [a]	29.5	29.7
C17 [a]	33.3	30.4
C5 [b]	38.0	35.7
C2 [b]	39.2	36.4
C10	46.4 [c]	44.0
C13	55.1	52.0
C1	56.5	56.4
C15	58.3	57.0
CH_2–Et	59.8	61.9
C19–C23	125.1	124.2, 126.1, 126.5
C6–C9	127.7, 128.3	128.2
C3, C4	140.4, 141.2	140.1
C18	143.6	140.3
C12	166.8	168.2
C11	168.0	168.7
C24	173.0	169.7

[a,b] Assignments may be interchanged.
[c] Splitting of 33 Hz.

Table 7
Data referring to the crystal structure analysis of delapril

Formula	$C_{26}H_{33}ClN_2O_5$
Molecular weight	489.01
Crystal system	monoclinic
Space group	$P2_1$
a (Å)	16.098(5)
b (Å)	10.712(3)
c (Å)	7.856(2)
β (deg)	97.85(2)
V (Å^3)	1342.0(7)
Z	2
D_{calc} (g cm^{-3})	1.210
μ (cm^{-1})	1.787
$F(000)$	520
Measured reflections	3634 (3429 unique)
Reflections with $I > 2\sigma(I)$	2450 (2293 unique)
Reflections used in refinement	3429
Parameters refined	368
Max./min. height in final ΔF map (e Å^{-3})	0.17/−0.20
R^1 [a]	0.040
R_w^2 [b]	0.120

[a] $\Sigma||F_o|-|F_c||/\Sigma|F_o|$, calculated on observed reflections ($F_o > 4\sigma(F_o)$).
[b] $\{\Sigma[w(F_o^2-F_c^2)]^2/\Sigma(wF_o^2)^2\}^{1/2}$, for all data.

those belonging to the five-membered C1–C5 ring, which confirmed the sp^3 character of C2 and C5, were located by inspection of the ΔF map and refined isotropically. The remaining H atoms were introduced at calculated positions, riding on their carrier atoms, according to the protocols built in the refinement program. The correctness of the absolute configuration was confirmed by the value of Flack's parameter [28], which was refined according to SHELXL-93 protocol, giving the value of 0.12(9) for the enantiomer 13*S*,15*S*.

Table 8
Fractional atomic coordinates ($\times 10^4$) and equivalent isotropic displacement parameters (Å$^2 \times 10^4$) (one third of the trace of the diagonalized matrix), with the e.s.d. in parentheses for non-hydrogen atoms for delapril hydrochloride

Atom	X/a	Y/b	Z/c	U_{eq}
Cl	4019.9(7)	2789.1(8)	12291.2(12)	603(3)
O1	5855(2)	255(2)	5923(3)	550(9)
O2	6321(2)	1291(2)	8346(3)	508(8)
O3	4606(2)	2513(2)	7560(3)	465(8)
O4	3120(2)	6375(3)	7275(4)	621(10)
O5	2269(2)	5144(3)	5493(4)	777(12)
N1	5673(2)	3545(3)	6621(3)	395(8)
N2	3911(2)	4415(3)	8970(4)	417(9)
C1	6193(2)	4657(3)	6461(5)	451(11)
C2	7091(3)	4503(5)	7415(6)	633(15)
C3	7645(3)	4510(4)	6029(6)	635(15)
C4	7194(3)	4770(4)	4443(6)	626(15)
C5	6281(3)	4972(4)	4562(5)	568(14)
C6	7595(4)	4855(7)	2985(8)	1023(26)
C7	8451(5)	4644(10)	3160(12)	1406(41)
C8	8892(4)	4383(8)	4721(15)	1372(42)
C9	8504(3)	4313(6)	6181(10)	961(25)
C10	5846(3)	2409(3)	5713(4)	437(11)
C11	6034(2)	1277(3)	6828(4)	414(10)
C12	5002(2)	3486(3)	7473(4)	383(10)
C13	4758(2)	4650(3)	8402(5)	402(10)
C14	5371(3)	4907(4)	10019(5)	541(13)
C15	3187(2)	4151(3)	7603(5)	456(11)
C16	2494(3)	3460(4)	8379(5)	569(13)
C17	2062(3)	4239(5)	9607(6)	716(17)
C18	1402(3)	3530(5)	10393(6)	735(17)
C19	1604(4)	2952(6)	11966(7)	906(21)
C20	1004(6)	2333(7)	12730(9)	1180(33)
C21	205(6)	2259(9)	11889(13)	1432(43)
C22	−14(5)	2800(13)	10371(12)	1664(49)
C23	595(4)	3483(10)	9613(9)	1313(36)
C24	2870(2)	5372(4)	6790(5)	517(12)
C25	1851(3)	6204(6)	4602(8)	999(23)
C26	973(3)	5877(7)	4116(10)	1132(29)

Programs PARST95 [29], ZORTEP (L. Zsolnai, H. Pritzkow, University of Heidelberg, Germany, 1994), PLUTO (W.D.S. Motherwell, W. Clegg, University of Cambridge, UK, 1976) were used for analyzing and drawing the molecular structure and the crystal packing. Use was made of the packages of the Cambridge Structural Database.

All the calculations were performed on an ENCORE91 computer (Fort Lauderdale, FL). Final atomic coordinates are given in Table 8, whereas geometric parameters are in Table 9.

Powder X-ray diffraction patterns were recorded on a Philips PW 1050 diffractometer (Eindhoven, The Netherlands) by using Cu Kα radiation over the interval 5–35°/2θ (speed 1°/min).

^1H NMR and ^{13}C NMR spectra were obtained at 200.1 and 50.3 MHz in D_2O or DMSO-d_6 on a Bruker ACF 200 instrument (Karlsruhe, Germany). The variable-temperature study was performed in DMSO-d_6 in the range 296–365 K. Standard Bruker microprograms (DISNMR 1989) were

Table 9
Bond distances (Å) and angles (°) with the e.s.d. in parentheses for delapril hydrochloride

O1–C11	1.316(4)	C6–C7	1.385(10)
O2–C11	1.219(4)	C7–C8	1.359(13)
O3–C12	1.229(4)	C8–C9	1.381(13)
O4–C24	1.192(5)	C10–C11	1.502(5)
O5–C24	1.329(5)	C12–C13	1.523(5)
O5–C25	1.451(7)	C13–C14	1.523(5)
N1–C1	1.470(5)	C15–C16	1.532(6)
N1–C10	1.456(4)	C15–C24	1.512(6)
N1–C12	1.349(5)	C16–C17	1.514(7)
N2–C13	1.513(5)	C17–C18	1.505(7)
N2–C15	1.500(4)	C18–C19	1.381(7)
C1–C2	1.543(6)	C18–C23	1.359(7)
C1–C5	1.554(6)	C19–C20	1.376(11)
C2–C3	1.500(7)	C20–C21	1.365(12)
C3–C4	1.382(6)	C21–C22	1.329(14)
C3–C9	1.388(6)	C22–C23	1.418(13)
C4–C5	1.502(6)	C25–C26	1.456(7)
C4–C6	1.392(8)		
C24–O5–C25	117.8(4)	O1–C11–O2	124.3(3)
C10–N1–C12	115.1(3)	O3–C12–N1	121.6(3)
C1–N1–C12	125.7(3)	N1–C12–C13	118.4(3)
C1–N1–C10	119.1(3)	O3–C12–C13	119.9(3)
C13–N2–C15	117.6(3)	N2–C13–C12	107.9(3)
N1–C1–C5	112.6(3)	C12–C13–C14	111.6(3)
N1–C1–C2	112.2(3)	N2–C13–C14	106.9(3)
C2–C1–C5	106.7(3)	N2–C15–C24	108.9(3)
C1–C2–C3	104.9(3)	N2–C15–C16	110.0(3)
C2–C3–C9	128.4(4)	C16–C15–C24	111.4(3)
C2–C3–C4	111.3(4)	C15–C16–C17	114.2(3)
C4–C3–C9	120.2(4)	C16–C17–C18	113.3(4)
C3–C4–C6	120.6(5)	C17–C18–C23	121.2(5)
C3–C4–C5	111.8(4)	C17–C18–C19	120.0(5)
C5–C4–C6	127.6(4)	C19–C18–C23	118.8(5)
C1–C5–C4	104.3(3)	C18–C19–C20	120.8(6)
C4–C6–C7	118.3(6)	C19–C20–C21	119.2(8)
C6–C7–C8	120.9(7)	C20–C21–C22	121.7(9)
C7–C8–C9	121.4(10)	C21–C22–C23	119.2(9)
C3–C9–C8	118.6(5)	C18–C23–C22	120.2(6)
N1–C10–C11	115.2(3)	O5–C24–C15	109.4(3)
O2–C11–C10	125.5(3)	O4–C24–C15	124.4(4)
O1–C11–C10	110.2(3)	O4–C24–O5	126.1(4)
		O5–C25–C26	107.9(4)

employed for 2D $^{1}H,^{1}H$ COSY, 2D $^{1}H,^{13}C$ COSY, 2D $^{1}H,^{13}C$ COSY 'long range' and 2D phase-sensitive ^{1}H NOESY experiments.

The line-shape analysis was performed on the central lines of the CH_3–Et triplet resonances. Theoretical line shapes were calculated with the aid of an 'in-house' program. For the analysis the program requires: the chemical shifts of the protons, the populations, the half-height widths and the rate constants. These parameters were adjusted by trial and error so as to obtain the best fit between the experimental and theoretical curves.

The ^{13}C NMR solid state spectra were obtained with the cross-polarization magic angle spinning (CP-MAS) accessory on a Bruker CXP 300 instrument (Karlsruhe, Germany). The spectra were measured with a contact time of 2 ms, which was not optimized. The side bands were assigned by carrying out the experiments at two different spinning rates.

Acknowledgements

The authors are grateful to Dr Lorenza Carima and Mr Milco Lipreri (Chiesi Farmaceutici SpA) for technical support and to Dr Daniele Casarini (University of Bologna) and Dr Riccardo Percudani (University of Parma) for their contribution to the thermodynamic parameter analysis.

References

[1] Y. Oka, K. Nishikawa, A. Miyake, Jpn. Patent Appl. 57-179141 (1982).
[2] A.J. Reyes, New developments in the management of congestive heart failure with angiotensin-converting inhibitors, Am. J. Cardiol. 75 (Suppl.) (1995) 1–12.
[3] A.A. Patchett, E. Harris, E.W. Tristram, M.J. Wyvratt, M.T. Wu, D. Taub, E.R. Peterson, T.J. Ikeler, J. Broeke, L.G. Payne, D.L. Ondeyka, E.D. Thorsett, W.J. Greenlee, N.S. Lohr, R.D. Hoffsommer, H. Joshua, W.V. Ruyle, J.W. Rothrock, S.D. Aster, A.L. Maycock, F.M. Robinson, R. Hirschmann, C.S. Sweet, E.H. Ulm, D.M. Gross, T.C. Vassil, C.A. Stone, A new class of angiotensin-converting enzyme inhibitors, Nature 288 (1980) 280–283.
[4] M.J. Wyratt, A.A. Patchett, Recent developments in the design of angiotensin-converting enzyme inhibitors, Med. Res. Rev. 5 (1985) 483–531.
[5] H. Ito, M. Yasumatsu, Y. Usui, Determination of a new angiotensin-converting enzyme inhibitor and its metabolites in serum and urine by high performance liquid chromatography, Fukuoka Acta Med. 76 (1985) 441–450.
[6] E.G. Erdoes, The angiotensin I converting enzyme, Fed. Proc., Fed. Am. Soc. Exp. Biol. 36 (1977) 1760–1765.
[7] M.A. Ondetti, B. Rubin, D.W. Cushman, Design of specific inhibitors of angiotensin-converting enzyme: new class of orally active antihypertensive agents, Science 196 (1977) 441–444.
[8] J. Bernstein, in: G. Desiraju (ed.), Organic Solid State Chemistry, Studies in Organic Chemistry, vol. 32, Elsevier, Amsterdam, 1987, pp. 471–518.
[9] S. Byrn, Solid State Chemistry of Drugs, Academic Press, New York, 1982, pp. 99–103.
[10] D.W. Cushman, H.S. Cheung, E.F. Sabo, M.A. Ondetti, Design of potent competitive inhibitors of angiotensin-converting enzyme, carboxyalkanoyl and mercaptoalkanoyl aminoacids, Biochemistry 16 (1977) 5484–5491.
[11] E.D. Thorsett, E.E. Harris, S.D. Aster, E.R. Peterson, J.P. Snyder, J.P. Springer, J. Hirshfield, E.W. Tristram, A.A. Patchett, E.H. Ulm, T.C. Vassil, Conformationally restricted inhibitors of angiotensin-converting enzyme: synthesis and computations, J. Med. Chem. 29 (1986) 251–260.
[12] R.J. Hausin, P.W. Codding, Molecular and crystal structures of MDL27,467 A hydrochloride and quinapril hydrochloride, two ester derivatives of potent angiotensin-converting enzyme inhibitors, J. Med. Chem. 34 (1991) 511–517.
[13] C. Pascard, J. Guilhem, M. Vincent, G. Rémond, B. Portevin, M. Laubie, Configuration and preferential solid-state conformations of perindoprilat (S-9780). Comparison with the crystal structures of other ACE inhibitors and conclusions related to structure–activity relationships, J. Med. Chem. 34 (1991) 663–669.
[14] P.R. Andrews, J.M. Carson, A. Caselli, M.J. Spark, R. Woods, Conformational analysis and active site modelling of angiotensin-converting enzyme inhibitors, J. Med. Chem. 28 (1985) 393–399.

[15] G. Precigoux, S. Geoffre, F. Leroy, *N*-(1-ethoxycarbonyl-3-phenylpropyl)-L-alanyl-L-prolinium hydrogen maleate (1/1), enalapril maleate (MK-421), Acta Crystallogr. Sect. C 42 (1986) 1022–1024.
[16] M.J. Wyvratt, Reductive amination of ethyl 2-oxo-4-phenylbutanoate with L-alanyl-L-proline. Synthesis of enalapril maleate, J. Org. Chem. 49 (1984) 2816–2819.
[17] D. Rabenstein, A. Isab, Conformational and acid–base equilibria of Captopril in aqueous solution, Anal. Chem. 54 (1982) 526–529.
[18] D. Ip, G. Brenner, in: K. Florey (ed.), Analytical Profiles of Drugs, vol. 16, Academic Press, Orlando, FL, 1987, pp. 207–243.
[19] J. Sandström, Dynamic NMR Spectroscopy, Academic Press, London, 1982, pp. 96–99.
[20] D. Mayer, C.B. Naylor, I. Motoc, G.R. Marshall, A unique geometry of the active site of angiotensin-converting enzyme consistent with structure–activity studies, J. Comput. Aided Mol. Des. 1 (1987) 3–16.
[21] C. Pascard, Small molecules crystal structures as a structural basis for drug design, Acta Crystallogr. Sect. D 51 (1995) 407–417.
[22] W.A. Thomas, I.W.A. Whitcombe, Nuclear magnetic resonance studies and conformational analysis of bicyclic inhibitors of angiotensin-converting enzyme. Part 2. The octahydro-6H-pyridazo-[1,2-a][1,2]diazepine, J. Chem. Soc., Perkin Trans. 2 (1986) 747–755.
[23] P. Luger, G. Scnorrenberg, A highly potent angiotensin-converting enzyme inhibitor: (*S,S,S'*)-5-[*N*-(1-carboxy-3-phenylpropyl)-alanyl]-4,5,6,7-tetrahydrotieno[3,2c]pyridine-4-carboxylic acid monohydrate, SBG 107, Acta Crystallogr. Sect. C 43 (1987) 484–488.
[24] E.F. Paulus, R. Henning, H. Urbach, Structure of the angiotensin-converting enzyme inhibitor ramiprilat (HOE 498 diacid), Acta Crystallogr. Sect. C 43 (1987) 941–945.
[25] M. Vincent, C. Pascard, M. Cesario, G. Rémond, J.P. Bouchet, Y. Charton, M. Laubie, Synthesis and conformational studies of Zabicipril (S 9650-3), a potent inhibitor of angiotensin-converting enzyme, Tetrahedron Lett. 33 (1992) 7369–7372.
[26] S.J. Opella, J.G. Exem, M.H. Frey, T.A. Cross, Solid state n.m.r. of biopolymers, Phil. Trans. R. Soc. London Ser. A 299 (1984) 665–683.
[27] A. Altomare, G. Cascarano, C. Giacovazzo, A. Guagliardi, M.C. Burla, G. Polidori, M. Camalli, SIR 92 a program for automatic solution of crystal structures by direct methods, J. Appl. Crystallogr. 27 (1994) 435.
[28] H.D. Flack, An enantiomorph-polarity estimation, Acta Crystallogr. Sect. A 39 (1983) 876–881.
[29] M. Nardelli, PARST95: an update to PARST — a system of Fortran routines for calculating molecular structure parameters from the results of crystal structure analysis, J. Appl. Crystallogr. 28 (1995) 659.